



Bubble Based Micromanipulators in Microfluidics Systems: A Mini-review

Yuting Zhou^{1,2,3}, Ligu Dai⁴, Niandong Jiao^{1,2(✉)}, and Lianqing Liu^{1,2}

¹ State Key Laboratory of Robotics, Shenyang Institute of Automation, Chinese Academy of Sciences, Shenyang 110016, China

ndjiao@sia.cn

² Institutes for Robotics and Intelligent Manufacturing, Chinese Academy of Sciences, Shenyang 110016, China

³ University of Chinese Academy of Sciences, Beijing 100049, China

⁴ College of Mechanical and Electrical Engineering, Zhengzhou University of Light Industry, Zhengzhou 450002, China

Abstract. Bubbles in liquid have the advantages of controllability, compressibility and biocompatibility, so they are introduced into microfluidic system to drive the fluid and operate micro-objects including cells. In recent years, the acoustic and optothermal bubbles are the two most widely used and efficient bubbles in microfluidic devices. Therefore, the aim of this study is to review recent advances in acoustic bubble-based micromanipulators and optothermal bubble-based micromanipulators in microfluidic systems. The principles and applications of fluid control and micro-object operation of these two kinds of bubble-based manipulators are introduced and the prospects and challenges are discussed.

Keywords: Acoustic bubble · Optothermal bubble · Fluid control · Micro-objects manipulation

1 Introduction

In the microfluidic devices, the Reynolds number of fluid is much smaller than that of macro fluid, which makes the driving of microfluidic more difficult, as well as the operation of micro-objects. Based on the principle of bubble induced acoustic microstreaming, liquid flow can be promoted and controlled by microbubbles, and micro-objects can be operated under the action of Stokes drag force and Bjerknes force in different microstreaming patterns. In addition, the volume change of optothermal bubbles in the process of growth and disappearance will trigger the flow field, which can realize the control of the fluid. Under the combined action of Marangoni effect and balance between surface tension and pressure force, microparticles can be captured on the surface of optothermal bubbles and move with the movement of bubbles, and the microstructures can be pushed to the specified position and adjusted to expected three-dimensional (3D) gesture. In this review, we introduce and discuss recent advances in bubble-based micromanipulators in microfluidic systems. In Sect. 2.1 and Sect. 2.2, we introduce the

working principle, flow control and micro-object manipulation of the acoustic bubble-based manipulator and optothermal bubble-based manipulator, respectively. Finally, we summarize the current limitations of these two bubble-based manipulators and discuss the future development.

2 Results and Discussion

2.1 Acoustic Bubble-Based Manipulator

Working Principle. Acoustic oscillating bubbles include inertial and non-inertial cavitations [1]. Inertial cavitation means that the bubble expands and shrinks sharply or even collapses when the oscillation amplitude is high enough and above a certain threshold. Most oscillating bubbles in microfluids are stable, non-inertial cavitation bubbles. Oscillating bubbles have their natural frequencies, and when they have the same frequency as the exciting acoustic field, the bubbles will reach a maximum vibration amplitude. In microfluidic devices, most acoustic bubbles are trapped in the tube or microchannel and play a role. The resonance frequency f_0 of the bubble in the tube or microchannel is

$$f_0 = \frac{1}{2\pi} \sqrt{\frac{\kappa P_0}{\rho L_0 L_B}} \quad (1)$$

where κ is the polytropic index, P_0 is the constant far-field pressure, ρ is the density of the fluid around the bubble, and L_0 and L_B are the lengths of the liquid in the tube and the bubble column respectively. The microbubbles resonate under the action of acoustic wave, the contact surface between microbubbles and surrounding liquid will vibrate, which will trigger microstreaming and change the flow direction and speed of microfluids with different acoustic excitation frequency [2]. Ahmed et al. found that using ultrasound to oscillate bubbles trapped in a “horse-shoe” structure inside microtubules can affect fluid flow (Fig. 1a) [3]. With the different size and shape of bubbles, the flow microstreaming excited by acoustic bubbles is also different. Therefore, acoustic microbubbles are used to fabricate micromixer, micropump and microvalve.

In addition to manipulating microfluidics, acoustic bubbles can also manipulate particles and micro-objects such as cells. The particle close to the acoustic bubble is affected by two forces at the same time (Fig. 1b) [4]. One is the viscous resistance caused by the streamline direction of the micro flow field, that is, Stokes drag force f_d

$$f_d = 6\pi\eta R_P v_P \quad (2)$$

where η is the dynamic viscosity, R_P is the radius of the particle, and v_P is the flow velocity of solvent relative to the particles, which is also depend on R_P . The other is Bjerknes force f_R caused by the scattering effect of the bubble on the incident acoustic wave, also known as the second radiation force, for a rigid spherical particle

$$f_R = 4\pi\rho \frac{\rho - \rho_P}{\rho + 2\rho_P} \frac{R_b R_P}{d^5} \omega^2 \varepsilon^2 \quad (3)$$

where ρ is the density of the fluid of the fluid around the bubble, ρ_P is the density of particles, R_b is the instantaneous radii of a bubble, d is the distance between the

bubble and particle centres, ω is the angular frequency and ε is the bubble amplitude. Under different excitation frequencies, the flow field patterns around acoustic bubbles are different. By changing the magnitude of these two forces, a variety of motion patterns of particles can be realized, including capture, rotation and revolution.

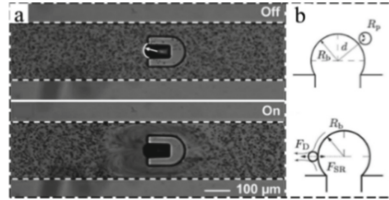


Fig. 1. (a) The acoustic streaming pattern around a bubble located in the horse-shoe structure of the microfluidic pipe. Adapted from Ahmed et al. [3] with permission from Royal Society of Chemistry, Copyright 2009. (b) The geometry and force analysis diagram of the particle trapped on the surface of the microbubble. Adapted from Chen et al. [4] with permission from Royal Society of Chemistry, Copyright 2016.

Flow Control. Cavitation microstreaming generated by acoustic bubbles can enhance fluid mixing, and the induced flow field and mixing intensity can be changed by changing the number [3], position and shape [5], arrangement and mixing area [6] of bubbles in the microfluidic pipe. Orbay et al. [7] introduced an acoustic-bubble based micromixer where the uniform mixing of two high viscosity liquids with low Reynolds number can be realized. Bertin et al. prepared an armoured microbubbles (AWBs) to overcome the problem of short service life of microbubbles [6]. Recently, Conde et al. [8] proposed a hybrid approach combining a substrate with a slab, in which the substrate contained mixing chamber and microfluidic channel, and the slab contained the structure required to capture bubbles (Fig. 2a). This method reduces the acoustic energy lost on the substrate and further improves the mixing efficiency. Micropump based on acoustic oscillation microbubbles have attracted extensive attention because of their simple structure and high specificity [9]. Patel and colleagues proposed a bubble-based micropump [10]. The bubbles in lateral cavity acoustic transducers (LCATs) produce oscillating flow velocity due to the oscillating movement of the air/liquid interface. This structure can separate particles or cells of different sizes. Recently, Gao et al. [11] placed opposite microcavity in the main microchannel to realize efficient bidirectional micropump (Fig. 2b). The flow direction of fluid and particles can be changed by actuating specific microbubbles of opposite directions and different sizes with different acoustic field driving frequencies. As for microvalve, acoustic bubbles can be used to adjust the chemical concentration as a chemical switch [12]. Ahmed et al. utilized the acoustic oscillating bubbles to generate digital chemical waveforms and analog waveforms, and the shape, frequency, amplitude and duty cycle can be easily modulated at the same time. It's a powerful tool for the investigation and characterization of the dynamic properties of many biochemical processes. (Fig. 2c) [13]. Similarly, Liu et al. [14] proposed a tunable chemical gradient generator based on the gas permeability of polydimethylsiloxane (PDMS). The adjustable chemical gradient was realized by changing the excitation combination of bubbles in different

channels. In general, the microstreaming generated by acoustic oscillation bubbles can be driven far beyond Stokes boundary layer, and can produce effective fluid control even when dealing with high viscosity fluids. In addition, such acoustic bubble fluid controllers are generally economical and low power consumption.

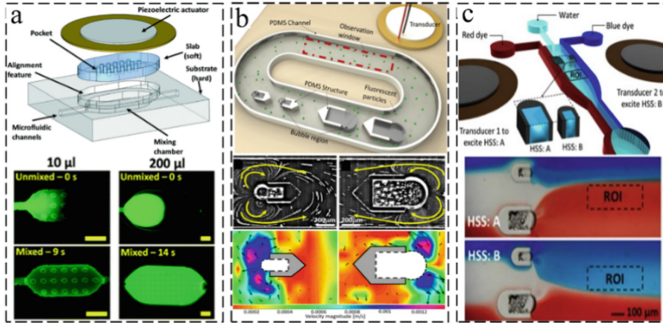


Fig. 2. (a) Up: configuration of the hybrid micromixer. Down: micrographs showing before and after mixing. Adapted from Conde et al. [8] with permission under the terms of CC BY 3.0 license, Copyright 2016. (b) Up: configuration of the acoustic-based bidirectional micropump device. Down: acoustic bubble induced microstreaming flow and the velocity profile given by particle image velocimetry (PIV). Adapted from Gao et al. [11] with permission from Springer Nature, Copyright 2020. (c) Up: schematic of the experimental setup for chemical switching. Down: results demonstrating switching between the blue and red dyes. Adapted from Ahmed et al. [13] with permission under the terms of ACS Author Choice License, Copyright 2014. (Color figure online)

Micro-object Manipulation. The microstreaming caused by oscillating bubbles (inertial and non-inertial) excited by acoustic field can make cell lysis, perforation and deformation. Low intensity ultrasound leads to stable cavitation of microbubbles, which is conducive to the cell formation of small pores and endocytosis. High intensity ultrasound can lead to inertial cavitation and bubble collapse, resulting in cell membrane perforation. In 2019, Meng et al. [15] utilized acoustic microbubbles oscillated with almost the same amplitude and resonance frequency to ensure efficient and uniform acoustic perforation. Recently, Liu et al. [16] realized efficient cell lysis on lab-on-a-chip (LOC) device by using acoustic driven oscillating bubble array. Subsequently, they fabricated a microfluidic device where the cells can be captured and paired with the oscillating bubble surface under acoustic excitation, further realizing the fusion of homotypic or heterotypic cell membranes [17]. Recently, they designed a traveling surface acoustic wave (TSAW) device composed of TSAW chip and PDMS channel to explore single-cell ultrasonic perforation using targeted microbubbles (TMB) in non-cavitation (Fig. 3a) [18]. TSAW was applied to accurately manipulate the movement of TMBs attached to MDA-MB-231 cells, resulting in ultrasonic deformation and reversible perforation at the single cell level.

In microfluidic devices, microbubbles can capture, rotate and operate cells under acoustic excitation through the joint action of Stokes force and Bjerknes force. In these

examples, bubbles are usually spontaneously generated due to the hydrophobicity of the structure and trapped in microchannels or microcavities. Ahmed et al. and Ozcelik et al. proposed a technique of acoustofluidic rotational manipulation (ARM) based on the oscillating bubbles trapped within sidewall microcavities of the microfluidic channel to realize the rotation of nematodes, single cells and organisms [19, 20]. Läubli et al. used similar methods to rotate plant cells to achieve high-resolution 3D reconstruction [21]. Tang et al. then realized the 3D reconstruction of HeLa cells [22]. Peng [23] manufactured a microfluidic device where the particles can be focused, captured, extracted and enriched in a non-contact, unmarked and continuous manner by activating bubbles at a specific frequency. Recently, Gao et al. [24] captured bubbles with the required size and position in the microcavity structure of monolayer PDMS microchannels. In the low-frequency acoustic field, the oscillating motion of bubbles induced microfluidic vortices, which were used to break blood clots in blood samples (Fig. 3b). Then, they proposed a tumor-on-a-chip platform (ABSTRACT platform) based on acoustic oscillating bubbles to capture and rotate CTCs to the desired position [25].

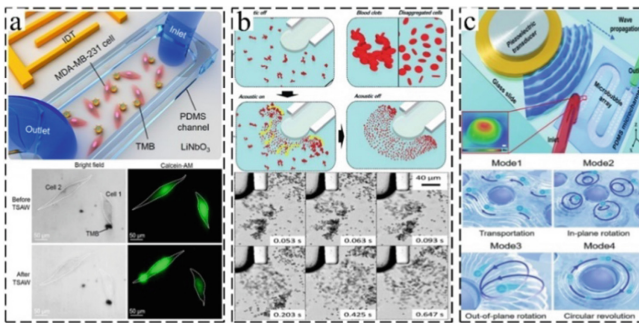


Fig. 3. (a) Up: schematic of the experimental device. Down: bright field and calcein-AM images of the sonoporation achieved before and after the TSAW treatment. Adapted from Liu et al. [18] with permission under the terms of CC BY 4.0 license, Copyright 2022. (b) Up: working mechanism of acoustic bubble-based thrombolysis. Down: blood clots disaggregated to single cells by the acoustically excited bubble. Adapted from Gao et al. [24] with permission from Royal Society of Chemistry, Copyright 2021. (c) Up: schematic of the acoustofluidic multimodal manipulation device. Down: diverse modes of acoustic microstreaming and sample manipulation. Adapted from Zhang et al. [26] with permission from Royal Society of Chemistry, Copyright 2021.

Acoustic bubbles in microfluidic devices can also realize particle and cell sorting. Rogers et al. [27] selectively captured particles by acoustically excited oscillating bubbles. According to the size and resonance frequency of the bubbles, the interaction between Stokes force and Bjerkness force was different, resulting in particle attraction or repulsion. Recently, Meng et al. [28] effectively separate two cells with the same size distribution through surface acoustic waves and targeted microbubbles. By specifically adhering targeted microbubbles to MDA-MB-231 cells, the acoustic sensitivity of the cells can be significantly improved, so that MDA-MB-231 cells can be separated from MCF-7 cells. Acoustically excited oscillating bubbles can also realize the transmission

and multiple manipulation of particles. Xie et al. [29] controlled the trajectory of particles in a LOC device by using oscillating bubbles trapped in “horseshoe” structure. Once the bubble was excited and oscillated, the particles would be captured by adjacent bubbles. After the transducer was shut down again, the particles immediately returned to the laminar driving state. Recently, Zhang et al. [26] proposed a multifunctional bubble-based acoustofluidic device. By changing the applied acoustic field frequency, the arranged bubbles trapped in the microcavity at the bottom of the chip can be flexibly switched between four different oscillatory motions, so as to generate corresponding microstreaming modes in the microchannel and realize the stable transportation, trapping, 3D rotation and circular revolution of micro-objects (Fig. 3c). In general, due to the different oscillation states and corresponding microfluidic modes of acoustic bubbles, they can achieve a variety of controllable multimodal operations on micro-objects, and has a wide range of applications in the biological field.

2.2 Optothermal Bubble-Based Manipulator

Working Principle. The optothermal effect is usually used to convert light energy into heat energy, and microbubbles are generated at the interface between heat absorbing materials (including metal, amorphous silicon, indium tin oxide or their combination) and liquid [30]. The temperature decreased along the radial direction because of convective cooling along the top and bottom surfaces. This temperature gradient causes a corresponding convective flow which forms a clockwise flow pattern near the bubble–liquid interface (Fig. 4a) [31]. This microscale circulation is caused by the Marangoni effect. The velocity field between liquid layers caused by the thermal Marangoni effect can be described as [32]

$$\eta \left(\frac{\partial \mu}{\partial \mathbf{n}} \right) = \gamma_T \left(\frac{\partial \mathbf{T}}{\partial \mathbf{t}} \right) \quad (4)$$

where η is the dynamic viscosity, μ is the tangential component of the fluid velocity vector at the interface between liquid and air, and \mathbf{n} and \mathbf{t} are the unit vectors of the normal and tangential directions of the interface, respectively. $\gamma_T = \partial \gamma / \partial T$ is the derivative of surface tension γ with respect to temperature.

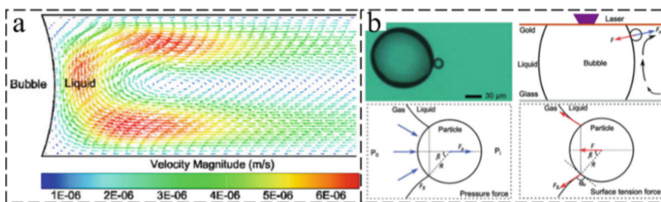


Fig. 4. (a) Convective flow pattern around an optothermal bubble. (b) The experimental image and force analysis image when a particle is trapped on the bubble surface. Adapted from Zhao et al. [31] with permission from Royal Society of Chemistry, Copyright 2014.

Under the action of Marangoni convection, the particles will be brought to the bubble, and will finally be captured on the bubble surface. The force balance on the particle located at the bubble–liquid interface can be described as (Fig. 4b) [31]

$$\frac{F}{F_P} = \frac{R_B \sin(|\theta_C - \beta|)}{R \sin\beta} \quad (5)$$

where F is the combined force of the surface tension F_S , F_P is the pressure force, R_B is the radius of the bubble and R is the radius of the particle, θ_C is the contact angle among the particle and the liquid–gas interface, and β is the half central angle. The balance between these two forces keeps the particles tightly trapped on the bubble surface, and makes it possible for optothermal bubbles to manipulate other micromodules.

Flow Control. The liquid jet produced by cavitation bubble collapse can cause different fluid mixing. In 2007, Hellman et al. utilized laser to produce cavitation bubbles in the microfluidic channel solidified with silicone resin, which realizes the mixing of water and naphthol green dye. For micropump, Dijkink et al. first produced a pump based on the principle of cavitation bubbles generated by laser pulse focusing to drive the flow of microfluidic fluid [33]. As for the microvalve, the bubble can play the role of a valve in the microfluidic system using the characteristic that the bubble volume is affected by temperature. In 2011, Zhang et al. [34] used laser to irradiate the chromium pad immersed in the liquid to produce controllable bubbles, and control the flow direction of the fluid through the growth process of bubbles, which could realize the open and closed state of laminar flow as a microvalve (Fig. 5a). Subsequently, Jian et al. [35] used laser-induced bubbles to selectively control the flow direction in microfluidic chips. The direction and speed of the pumping flow can be adjusted by changing the spot position and laser power. In order to reduce the complexity of optical system, Hyun et al. [36] deposited titanium film on the roughened end-face of silica optical fiber to make optic fiber microheater, and embedded it into microfluidic system to form an optofluidic microvalve-on-a-chip system. The high-speed bubble can grow into a vapor plug, which successfully blocks the liquid flow in the microchannel as a valve. Compared with the acoustic bubble fluid controller, the advantage of the optothermal bubble fluid controller is that it can generate bubbles at almost any position of the microchannel to realize the fluid control of specific parts. However, its disadvantage is that a laser beam can only generate one optothermal bubble, which has a relatively low efficiency; and the equipment is more expensive and complex.

Micro-object Manipulation. When the laser pulse is focused on the buffer interface of the cell solution, local cavitation bubbles will be generated. The hydrodynamic force induced by bubble expansion and subsequent collapse will cause the rupture of cell membrane. Rau et al. analyzed the operation mechanism and hydrodynamics behind the pulsed laser microbeam-induced cell lysis [37]. They found that cavitation bubble expansion was the primary agent of cell lysis. Cavitation bubble collapse, jet formation, and subsequent radial outflow of fluid can also result in the lysis of cells in the central region. Li et al. [38] designed conversion structures to capture a single cell, and then a single cavitation bubble was generated next to a single captured cell by laser. The jet generated by the collapse of the cavitation bubble was directed to the cell, resulting

in strong deformation and lysis. Hu et al. utilized the laser to intermittently irradiate the chip to produce bubbles to move cells [39]. With the movement of the laser, the bubbles generated by the last laser irradiation will quickly separate from the substrate and cause optothermal capillary flow. This micro flow will drive the cells to move a certain distance, and the continuous generation and floating bubbles can continuously move the operated cell. Thus, the damage of optothermal bubble temperature to cells is greatly reduced. Fan et al. used the oscillation of bubble volume in the opening and closing cycle of laser pulse to generate shear stress on the cell membrane near the bubble, so as to realize cell perforation [40, 41]. Subsequently, they integrated a single-cell analysis platform for cell perforation, cell lysis and cell manipulation (Fig. 5b) [42]. In microfluidic chips, optothermal bubbles can screen small objects. For example, Wu et al. reported a high speed and high purity pulsed laser triggered fluorescence activated cell sorter (PLACS) (Fig. 5c) [43]. They used the pulsed laser controlled by the detector to generate explosive vapor microbubbles in the outer channel and trigger a high-speed jet in the sample channel, which can make the specific cells deviate from the original path and enter the collection channel to realize the cell sorting function.

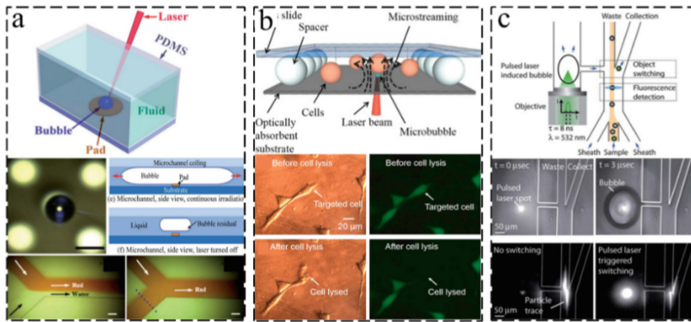


Fig. 5. (a) Up: illustration of bubble generation on the chromium pad. Down: experimental image of bubble growth, an illustration of the bubble behavior and the laser-induced bubble acts as a microvalve. Adapted from Zhang et al. [34] with permission from Royal Society of Chemistry, Copyright 2011. (b) Up: 3D structure of the microfluidic chamber where the cells can be cultured and lysed. Down: brightfield images and fluorescent images before and after the adherent single-cell lysis. Adapted from Fan et al. [42] with permission under the terms of CC BY 4.0 license, Copyright 2017. (c) Up: schematic of the cell sorter. Down: time-resolved images of the laser-induced cavitation bubble and fluorescent particle switching in PLACS. Adapted from Wu et al. [43] with permission from Royal Society of Chemistry, Copyright 2012.

Optothermal bubbles can also manipulate microstructure. Hu et al. utilized optothermal bubbles to realize the movement and arrangement of multiple triangular SU-8 structures, and assembled the hydrogel structures with cells inside into a specific array. Researchers have further developed a system that can generate and move multiple optothermal bubbles at the same time (Fig. 6a) [44]. Cooperation between optothermal bubbles improves the efficiency of moving and operating micromodules. Therefore, optothermal bubble microrobot has a wide application potential in biomedicine and tissue engineering. However, the process of biological tissue reconstruction is complex.

Due to the limitations of the generation and movement of optothermal bubbles in the two-dimensional (2D) plane of the solid-liquid interface, optothermal bubbles can only move the hydrogel structure, but cannot adjust the 3D posture of a single hydrogel structure, which limits the real application in the construction of biological tissue engineering. Fukuda et al. utilized a needle tube to blow bubbles into the solution, and the flow field driven by the bubbles floating in the fluid made the hollow hydrogel module with cell structure float up (Fig. 6b) [45, 46]. They used another needle tube to string up the micromodules. After repeating this action, they string up a series of hydrogel modules with different shapes, and again used the generated bubbles to adjust the posture of the micromodules to make them arranged neatly. Although this method realized the 3D operation of the micromodule, it needs two actuators to control the injection and collection at the same time, which has complex mechanical structure and high control difficulty. Moreover, the collected micromodules must have holes in the center to string to the collector. In order to solve the above problems, Dai et al. creatively proposed a method to utilize the optothermal bubbles on the 2D surface to realize the 3D arrangement and assembly of the hydrogel microstructure (Fig. 6c) [47]. By controlling the position and size of the optothermal bubbles generated at the bottom of the micromodule, they can lift, flip and flexibly adjust the 3D posture of the micromodule. They assembled the hollow ring structure into a 3D vascular structure and nested two ring modules of different sizes. Then, Ge of the same research group utilized the optothermal bubble operation method proposed by Dai to assemble the cell loaded microstructure into a peritoneal tissue structure highly similar to biological peritoneum, which verified the biocompatibility and feasibility of this method [48]. On this basis, Dai et al. further utilized the 3D operation ability and cluster cooperation ability of bubble microrobots to

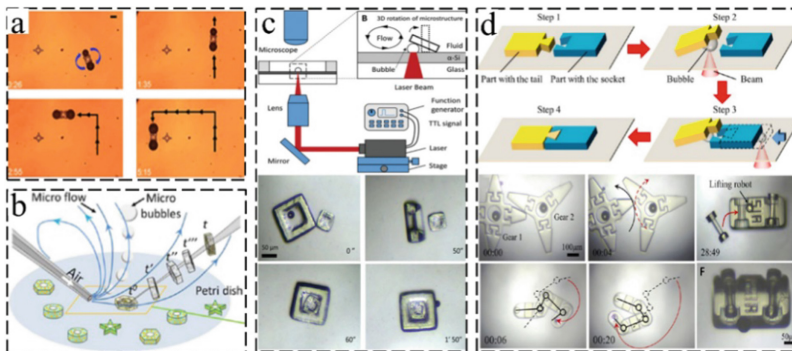


Fig. 6. (a) Micromanipulation of a microstructure using a pair of optothermal bubbles. Adapted from Rahman et al. [44] with permission under the terms of CC BY 4.0 license, Copyright 2017. (b) Schematic of the pickup of micromodules based on microbubble injection. Adapted from Wang et al. [46] with permission from American Chemical Society, Copyright 2017. (c) Up: schematic of the system setup to generate optothermal bubbles. Down: 3D manipulation and assembly of square ring microstructures. Adapted from Dai et al. [47] with permission from John Wiley and Sons, Copyright 2019. (d) Up: schematic of the integrated assembly process of two microparts by optothermal bubbles. Down: the assembled gears, snake-shaped structure and car. Adapted from Dai et al. [49] with permission from American Chemical Society, Copyright 2020.

realize the assembly of multiple micromodules with different interfaces, including mortise and tenon, gear, chain and car, which provided a new solution for the manufacturing, assembly and driving of micro/nanostructure (Fig. 6d) [49]. In general, the optothermal bubbles can realize diversified operation and different forms of motion states of a single micro-object more flexibly and controllably, and plays an important role in the field of precision microoperation and modular assembly.

3 Summary and Outlook

In this mini-review, the basic theory and wide applications of acoustic bubbles and optothermal bubbles manipulators in microfluidic devices were discussed. Bubbles are a double-edged sword in the microfluidic system. Free and uncontrolled bubbles can cause damage, but bubbles under the control of the energy field can become a favorable tool in microfluidic system. Bubble-based manipulators still have great development space in microfluidics. We will further discuss its challenges and future development.

For the acoustic bubble-based manipulator, it has the characteristics of simple equipment, easy implementation, low power consumption and low cost. However, under the long-time oscillation of the gas-liquid interface, the gas in the bubble may dissolve, resulting in changes in the size and shape of the bubble. The resonance frequency of the bubble can be affected, which may lead to the failure of the operation function. Therefore, how to extend the service life of bubbles and improve the effectiveness and stability of the bubble operation is an urgent problem to be solved in future development. For the optothermal bubble-based manipulator, it has high flexibility and controllability. However, the high temperature generated in the laser irradiation area may cause damage to cells and biomolecules, which limits the relevant biological applications. The latest breakthrough of optothermal bubbles is to realize the 3D manipulation and assembly of microstructure on 2D plane [47, 49], which is difficult to realize without relying on other operation technology such as microgripper/micropipette. Moreover, feedback control can be easily combined with the laser-induced optothermal bubbles to realize the automatic operation and the cooperative control of bubbles, which is expected to realize an operation factory.

In conclusion, the action range of the manipulator based on acoustic bubble and optothermal bubble is limited to the 2D plane. Although they can be combined with other operators such as microgripper [50] and magnetic microrobot [51] to complete operation tasks in 3D space, the mechanical structure becomes more complex and is only suitable for an open chip. The combination by superimposing multiple physical fields may further improve the control performance of bubbles. Researchers have combined acoustic-magneto [51], light-acoustic [52] to further expand the application range of bubble-based manipulator, and we look forward to the combination of multiple physical fields to provide more possibilities. The bubble manipulator microfluidics has great application value in biomedicine, microfluidics, clinical application and chemistry, which needs more scholars to study. We hope that in the future, bubble-based manipulators in microfluidic systems can integrate capture, transport and functional applications of micro-objects, just like an automatic assembly line.

Acknowledgement. This work is supported by the National Natural Science Foundation of China (Grant Nos. 91748212, U1613220, 91848201), and the CAS/SAFEA International Partnership Program for Creative Research Teams.

References

1. Hashmi, A.: Oscillating bubbles: a versatile tool for lab on a chip applications. *Lab Chip* **12**(21), 4216–4227 (2012)
2. Patel, M.V.: Lateral cavity acoustic transducer as an on-chip cell/particle microfluidic switch. *Lab Chip* **12**(1), 139–145 (2012)
3. Ahmed, D.: A millisecond micromixer via single-bubble-based acoustic streaming. *Lab Chip* **9**(18), 2738–2741 (2009)
4. Chen, Y.: Onset of particle trapping and release via acoustic bubbles. *Lab Chip* **16**(16), 3024–3032 (2016)
5. Ozelcik, A.: An acoustofluidic micromixer via bubble inception and cavitation from microchannel sidewalls. *Anal. Chem.* **86**(10), 5083–5088 (2014)
6. Bertin, N.: Bubble-based acoustic micropulsors: active surfaces and mixers. *Lab Chip* **17**(8), 1515–1528 (2017)
7. Orbay, S.: Mixing high-viscosity fluids via acoustically driven bubbles. *J. Micromech. Microeng.* **27**(1), 015008 (2017)
8. Conde, A.J.: Versatile hybrid acoustic micromixer with demonstration of circulating cell-free DNA extraction from sub-ml plasma samples. *Lab Chip* **20**(4), 741–748 (2020)
9. Tovar, A.R.: Lateral cavity acoustic transducer. *Lab Chip* **9**(1), 41–43 (2009)
10. Patel, M.V.: Cavity-induced microstreaming for simultaneous on-chip pumping and size-based separation of cells and particles. *Lab Chip* **14**(19), 3860–3872 (2014)
11. Gao, Y., Wu, M., Lin, Y., Zhao, W., Xu, J.: Acoustic bubble-based bidirectional micropump. *Microfluid. Nanofluid.* **24**(4), 1 (2020). <https://doi.org/10.1007/s10404-020-02334-6>
12. Ahmed, D.: Tunable, pulsatile chemical gradient generation via acoustically driven oscillating bubbles. *Lab Chip* **13**(3), 328–331 (2013)
13. Ahmed, D.: Acoustofluidic chemical waveform generator and switch. *Anal. Chem.* **86**(23), 11803–11810 (2014)
14. Liu, B.: A concentration gradients tunable generator with adjustable position of the acoustically oscillating bubbles. *Micromachines* **11**(9), 827 (2020)
15. Meng, L.: Sonoporation of cells by a parallel stable cavitation microbubble array. *Adv. Sci. (Weinh.)* **6**(17), 1900557 (2019)
16. Liu, X.: Cell lysis based on an oscillating microbubble array. *Micromach. (Basel)* **11**(3), 288 (2020)
17. Liu, X.: Rapid cell pairing and fusion based on oscillating bubbles within an acoustofluidic device. *Lab Chip* **22**(5), 921–927 (2022)
18. Liu, X.: Non-cavitation targeted microbubble-mediated single-cell sonoporation. *Micromach. (Basel)* **13**(1), 113 (2022)
19. Ozelcik, A.: acoustofluidic rotational manipulation of cells and organisms using oscillating solid structures. *Small* **12**(37), 5120–5125 (2016)
20. Ahmed, D.: Rotational manipulation of single cells and organisms using acoustic waves. *Nat. Commun.* **7**, 11085 (2016)
21. Läubli, N.F.: 3D manipulation and imaging of plant cells using acoustically activated microbubbles. *Small Methods* **3**(3), 1800527 (2019)

22. Tang, Q., Liang, F., Huang, L., Zhao, P., Wang, W.: On-chip simultaneous rotation of large-scale cells by acoustically oscillating bubble array. *Biomed. Microdevice* **22**(1), 1–11 (2020). <https://doi.org/10.1007/s10544-020-0470-1>
23. Peng, T.: Trapping stable bubbles in hydrophobic microchannel for continuous ultrasonic microparticle manipulation. *Sens. Actuators A Phys.* **331**, 113045 (2021)
24. Gao, Y.: Study of ultrasound thrombolysis using acoustic bubbles in a microfluidic device. *Lab Chip* **21**(19), 3707–3714 (2021)
25. Gao, Y.: Acoustic bubble for spheroid trapping, rotation, and culture: a tumor-on-a-chip platform (ABSTRACT platform). *Lab Chip* **22**(4), 805–813 (2022)
26. Zhang, W.: Versatile acoustic manipulation of micro-objects using mode-switchable oscillating bubbles: transportation, trapping, rotation, and revolution. *Lab Chip* **21**(24), 4760–4771 (2021)
27. Rogers, P.: Selective particle trapping using an oscillating microbubble. *Lab Chip* **11**(21), 3710–3715 (2011)
28. Meng, L.: Microbubble enhanced acoustic tweezers for size-independent cell sorting. *Appl. Phys. Lett.* **116**(7), 073701 (2020)
29. Xie, Y.L.: Acoustofluidic relay sequential trapping and transporting of microparticles via acoustically excited oscillating bubbles. *JALA* **19**(2), 137–143 (2014)
30. Ohta, A.T.: Optically actuated thermocapillary movement of gas bubbles on an absorbing substrate. *Appl. Phys. Lett.* **91**, nihpa130823 (2007)
31. Zhao, C.: Theory and experiment on particle trapping and manipulation via optothermally generated bubbles. *Lab Chip* **14**(2), 384–391 (2014)
32. Higuera, F.J.: Steady thermocapillary-buoyant flow in an unbounded liquid layer heated nonuniformly from above. *Phys. Fluids* **12**(9), 2186–2197 (2000)
33. Dijkink, R.: Laser-induced cavitation based micropump. *Lab Chip* **8**(10), 1676–1681 (2008)
34. Zhang, K.: Laser-induced thermal bubbles for microfluidic applications. *Lab Chip* **11**(7), 1389–1395 (2011)
35. Jian, A.Q.: Microfluidic flow direction control using continuous-wave laser. *Sens. Actuators A Phys.* **188**, 329–334 (2012)
36. Kim, H.-T.: Optofluidic microvalve-on-a-chip with a surface plasmon-enhanced fiber optic microheater. *Biomicrofluidics* **8**(5), 054126 (2014)
37. Rau, K.R.: Pulsed laser microbeam-induced cell lysis: time-resolved imaging and analysis of hydrodynamic effects. *Biophys. J.* **91**(1), 317–329 (2006)
38. Li, Z.G.: Single cell membrane poration by bubble-induced microjets in a microfluidic chip. *Lab Chip* **13**(6), 1144–1150 (2013)
39. Hu, W.: An opto-thermocapillary cell micromanipulator. *Lab Chip* **13**(12), 2285–2291 (2013)
40. Fan, Q.: Laser-induced microbubble poration of localized single cells. *Lab Chip* **14**(9), 1572–1578 (2014)
41. Fan, Q.: Efficient single-cell poration by microsecond laser pulses. *Lab Chip* **15**(2), 581–588 (2015)
42. Fan, Q.: Localized single-cell lysis and manipulation using optothermally-induced bubbles. *Micromach. (Basel)* **8**(4), 121 (2017)
43. Wu, T.H.: Pulsed laser triggered high speed microfluidic fluorescence activated cell sorter. *Lab Chip* **12**(7), 1378–1383 (2012)
44. Rahman, M.A.: Cooperative micromanipulation using the independent actuation of fifty microrobots in parallel. *Sci. Rep.* **7**(1), 3278 (2017)
45. Zheng, Z.: 3D construction of shape-controllable tissues through self-bonding of multicellular microcapsules. *ACS Appl. Mater. Interfaces* **11**(26), 22950–22961 (2019)
46. Wang, H.: Assembly of RGD-modified hydrogel micromodules into permeable three-dimensional hollow microtissues mimicking in vivo tissue structures. *ACS Appl Mater Interfaces* **9**(48), 41669–41679 (2017)

47. Dai, L.: 2D to 3D manipulation and assembly of microstructures using optothermally generated surface bubble microrobots. *Small* **15**(45), e1902815 (2019)
48. Ge, Z.: Bubble-based microrobots enable digital assembly of heterogeneous microtissue modules. *Biofabrication* **14**(2), 025023 (2022)
49. Dai, L.: Integrated assembly and flexible movement of microparts using multifunctional bubble microrobots. *ACS Appl. Mater. Interfaces* **12**(51), 57587–57597 (2020)
50. Zhou, Y.: Soft-contact acoustic microgripper based on a controllable gas-liquid interface for biomicromanipulations. *Small* **17**(49), e2104579 (2021)
51. Giltinan, J.: Programmable assembly of heterogeneous microparts by an untethered mobile capillary microgripper. *Lab Chip* **16**(22), 4445–4457 (2016)
52. Xie, Y.: Probing cell deformability via acoustically actuated bubbles. *Small* **12**(7), 902–910 (2016)